AFRL-AFOSR-VA-TR-2016-0145

Quasi-continuum reduction of field theories: A route to seamlessly bridge quantum and atomistic length-scales with continuum

Vikram Gavini
UNIVERSITY OF MICHIGAN

04/01/2016
Final Report

Air Force Research Laboratory
AF Office Of Scientific Research (AFOSR)/ RTA2
Arlington, Virginia 22203
Air Force Materiel Command

REPORT DOCUMENTATION PAGE	*Form Approved* *OMB No. 0704-0188*

1. REPORT DATE *(DD-MM-YYYY)* 04-01-2016	**2. REPORT TYPE** Final Performance Report	**3. DATES COVERED** *(From - To)* 03-01-2013 - 02-29-2016

4. TITLE AND SUBTITLE Quasi-continuum reduction of field theories: A route to seamlessly bridge quantum and atomistic length-scales with continuum	**5a. CONTRACT NUMBER**
	5b. GRANT NUMBER FA9550-13-1-0113
	5c. PROGRAM ELEMENT NUMBER
6. AUTHOR(S) Vikram Gavini	**5d. PROJECT NUMBER**
	5e. TASK NUMBER
	5f. WORK UNIT NUMBER
7. PERFORMING ORGANIZATION NAME(S) AND ADDRESS(ES) The Regents of the University of Michigan, 3003 S. State Street, Room 1056, Ann Arbor, MI 48109-1274	**8. PERFORMING ORGANIZATION REPORT NUMBER** DRDA: 13-PAF00457
9. SPONSORING/MONITORING AGENCY NAME(S) AND ADDRESS(ES) Air Force Office of Scientific Research 875 N. RANDOLPH ST. ROOM 3112 ARLINGTON VA 22203	**10. SPONSOR/MONITOR'S ACRONYM(S)**
	11. SPONSOR/MONITOR'S REPORT NUMBER(S)

12. DISTRIBUTION/AVAILABILITY STATEMENT

Approved for Public Release; Distribution is Unlimited.

13. SUPPLEMENTARY NOTES

14. ABSTRACT

This report summarizes the research objectives achieved in this project during the period 03-01-2013 to 02-29-2016. Computational techniques have been developed that enable large-scale real-space electronic structure calculations using Kohn-Sham density functional theory. In particular, the various components of the developed techniques include (i) real-space formulation of Kohn-Sham density-functional theory (DFT) for both pseudopotential and all-electron calculations based on a finite-element discretization; (ii) development of efficient and scalable algorithms for the solution of the Kohn-Sham eigenvalue problem based on Chebyshev filtering; (iii) development of reduced- order scaling techniques by employing a subspace projection technique in conjunction with local- ization techniques that construct a non-orthogonal localized basis spanning the Chebyshev filtered subspace; (iv) leveraging the localized representation to construct the quasi-continuum reduction. Most aspects of these developments have been numerically implemented, and the benchmark stud- ies have demonstrated that the developed techniques significantly outperform existing conventional DFT implementations in terms of computational efficiency, scaling with system size, and parallel scalability of

15. SUBJECT TERMS

Density Functional theory, Real Space, Finite Elements , Reduced-order scaling, Localization techniques

16. SECURITY CLASSIFICATION OF:			**17. LIMITATION OF ABSTRACT**	**18. NUMBER OF PAGES**	**19a. NAME OF RESPONSIBLE PERSON**
a. REPORT	**b. ABSTRACT**	**c. THIS PAGE**			**19b. TELEPHONE NUMBER** *(Include area code)*
U	U	U	UU	1	

Reset

Standard Form 298 (Rev. 8/98)
Prescribed by ANSI Std. Z39.18
Adobe Professional 7.0

INSTRUCTIONS FOR COMPLETING SF 298

1. REPORT DATE. Full publication date, including day, month, if available. Must cite at least the year and be Year 2000 compliant, e.g. 30-06-1998; xx-06-1998; xx-xx-1998.

2. REPORT TYPE. State the type of report, such as final, technical, interim, memorandum, master's thesis, progress, quarterly, research, special, group study, etc.

3. DATES COVERED. Indicate the time during which the work was performed and the report was written, e.g., Jun 1997 - Jun 1998; 1-10 Jun 1996; May - Nov 1998; Nov 1998.

4. TITLE. Enter title and subtitle with volume number and part number, if applicable. On classified documents, enter the title classification in parentheses.

5a. CONTRACT NUMBER. Enter all contract numbers as they appear in the report, e.g. F33615-86-C-5169.

5b. GRANT NUMBER. Enter all grant numbers as they appear in the report, e.g. AFOSR-82-1234.

5c. PROGRAM ELEMENT NUMBER. Enter all program element numbers as they appear in the report, e.g. 61101A.

5d. PROJECT NUMBER. Enter all project numbers as they appear in the report, e.g. 1F665702D1257; ILIR.

5e. TASK NUMBER. Enter all task numbers as they appear in the report, e.g. 05; RF0330201; T4112.

5f. WORK UNIT NUMBER. Enter all work unit numbers as they appear in the report, e.g. 001; AFAPL30480105.

6. AUTHOR(S). Enter name(s) of person(s) responsible for writing the report, performing the research, or credited with the content of the report. The form of entry is the last name, first name, middle initial, and additional qualifiers separated by commas, e.g. Smith, Richard, J, Jr.

7. PERFORMING ORGANIZATION NAME(S) AND ADDRESS(ES). Self-explanatory.

8. PERFORMING ORGANIZATION REPORT NUMBER. Enter all unique alphanumeric report numbers assigned by the performing organization, e.g. BRL-1234; AFWL-TR-85-4017-Vol-21-PT-2.

9. SPONSORING/MONITORING AGENCY NAME(S) AND ADDRESS(ES). Enter the name and address of the organization(s) financially responsible for and monitoring the work.

10. SPONSOR/MONITOR'S ACRONYM(S). Enter, if available, e.g. BRL, ARDEC, NADC.

11. SPONSOR/MONITOR'S REPORT NUMBER(S). Enter report number as assigned by the sponsoring/ monitoring agency, if available, e.g. BRL-TR-829; -215.

12. DISTRIBUTION/AVAILABILITY STATEMENT. Use agency-mandated availability statements to indicate the public availability or distribution limitations of the report. If additional limitations/ restrictions or special markings are indicated, follow agency authorization procedures, e.g. RD/FRD, PROPIN, ITAR, etc. Include copyright information.

13. SUPPLEMENTARY NOTES. Enter information not included elsewhere such as: prepared in cooperation with; translation of; report supersedes; old edition number, etc.

14. ABSTRACT. A brief (approximately 200 words) factual summary of the most significant information.

15. SUBJECT TERMS. Key words or phrases identifying major concepts in the report.

16. SECURITY CLASSIFICATION. Enter security classification in accordance with security classification regulations, e.g. U, C, S, etc. If this form contains classified information, stamp classification level on the top and bottom of this page.

17. LIMITATION OF ABSTRACT. This block must be completed to assign a distribution limitation to the abstract. Enter UU (Unclassified Unlimited) or SAR (Same as Report). An entry in this block is necessary if the abstract is to be limited.

DISTRIBUTION A: Distribution approved for public release.

Final Report

Quasi-continuum reduction of field theories: A route to seamlessly bridge quantum and atomistic length-scales with continuum

Principal Investigator:
Vikram Gavini
Department of Mechanical Engineering
University of Michigan, Ann Arbor

Program Manager:
Dr. Jean-Luc Cambier
Computational Mathematics
Air Force Office of Scientific Research

Abstract

This report summarizes the research objectives achieved in this project during the period 03-01-2013 to 02-29-2016. Computational techniques have been developed that enable large-scale real-space electronic structure calculations using Kohn-Sham density functional theory. In particular, the various components of the developed techniques include (i) real-space formulation of Kohn-Sham density-functional theory (DFT) for both pseudopotential and all-electron calculations based on a finite-element discretization; (ii) development of efficient and scalable algorithms for the solution of the Kohn-Sham eigenvalue problem based on Chebyshev filtering; (iii) development of reduced-order scaling techniques by employing a subspace projection technique in conjunction with localization techniques that construct a non-orthogonal localized basis spanning the Chebyshev filtered subspace; (iv) leveraging the localized representation to construct the quasi-continuum reduction. Most aspects of these developments have been numerically implemented, and the benchmark studies have demonstrated that the developed techniques significantly outperform existing conventional DFT implementations in terms of computational efficiency, scaling with system size, and parallel scalability of the numerical implementation. We believe these developed techniques and the numerical implementation can aid as a platform for further development of scalable and efficient real-space Kohn-Sham DFT calculations on tens of thousands of atoms, and enable continuing efforts towards a seamless bridging of the quantum and continuum length-scales.

Summary of Research Objectives Achieved

In this project we have conducted a program of research to develop computational techniques that enable large-scale real-space Kohn-Sham DFT calculations which also form the basis for the quasicontinuum reduction that seamlessly bridge the quantum length-scale with the continuum and enable an accurate electronic structure study of defective crystals. A comprehensive summary of the important research objectives achieved in this project is presented below with references to the published articles (Motamarri et al., 2013; Iyer et al., 2014; Motamarri & Gavini, 2014, 2016).

1 Real-space formulation of Kohn-Sham DFT and finite-element discretization

1.1 Real-space formulation

The ground-state energy of a materials system in Kohn-Sham DFT is given by

$$E(\rho, \boldsymbol{R}) = T_{\rm s}(\rho) + E_{\rm xc}(\rho) + E_{\rm H}(\rho) + E_{\rm ext}(\rho, \boldsymbol{R}) + E_{\rm zz}(\boldsymbol{R})\,. \tag{1}$$

where ρ is the ground-state electron-density, $\boldsymbol{R} = \{\boldsymbol{R}_1, \boldsymbol{R}_2, \cdots, \boldsymbol{R}_{N_a}\}$ denotes the collection of nuclear positions in the system with the I^{th} nucleus having an atomic number Z_I. For sake of simplicity, we present the ideas in a non-periodic setting, but extension to periodic and semi-periodic problems is straightforward (as the formalism is in real-space) and has already been developed and implemented. In equation (1), the first term, $T_s(\rho)$, represents the kinetic energy of non-interacting electrons, the second term, $E_{\rm xc}(\rho)$, represents the exchange-correlation term which accounts for the quantum-mechanical interactions between electrons, and $\rho(\mathbf{x})$ represents the electron-density distribution. The last three terms of the energy functional (1) represent the classical electrostatic interactions—electron-electron, electron-nuclei and nuclei-nuclei interaction energies, respectively, and are given by:

$$E_H(\rho) = \frac{1}{2}\int\int \frac{\rho(\mathbf{x})\rho(\mathbf{x}')}{|\mathbf{x}-\mathbf{x}'|}\,d\mathbf{x}\,d\mathbf{x}' \;\;;\;\; E_{\rm ext}(\rho, \boldsymbol{R}) = -\sum_{I=1}^{N_a}\int \frac{Z_I\,\rho(\mathbf{x})}{|\mathbf{x}-\boldsymbol{R}_I|}\,d\mathbf{x} \;\;;\;\; E_{\rm zz}(\boldsymbol{R}) = \frac{1}{2}\sum_{\substack{I,J=1\\ J\neq I}}^{N_a} \frac{Z_I\,Z_J}{|\boldsymbol{R}_I - \boldsymbol{R}_J|}$$

The non-local (extended) electrostatic interactions involve the kernel $1/|\mathbf{r}-\mathbf{r}'|$, which is the Green's function of the Laplace operator. These electrostatic interactions are thus computed by taking recourse to the solution of the Poisson equation to evaluate the total electrostatic potential, $\varphi(\mathbf{x}, \boldsymbol{R})$, associated with the total charge distribution (Motamarri et al., 2012, 2013). Finally, the electron-density ρ and the kinetic energy of non-interacting electrons are computed from the self-consistent field (SCF) iteration of the Kohn-Sham eigenvalue problem which results from the first variation of the DFT energy functional in equation (1). The system of equations corresponding to the self-consistent formulation are:

$$\left(-\frac{1}{2}\nabla^2 + V_{\rm eff}(\rho, \boldsymbol{R})\right)\psi_i = \epsilon_i\psi_i, \quad V_{\rm eff}(\rho, \boldsymbol{R}) = \frac{\delta E_{\rm xc}}{\delta\rho} + \varphi(\rho, \boldsymbol{R}) \tag{2a}$$

$$2\sum_i f(\epsilon_i) = N_e; \quad \rho(\mathbf{x}) = 2\sum_{i=1}^{N} f(\epsilon_i)|\psi_i(\mathbf{x})|^2, \tag{2b}$$

$$-\frac{1}{4\pi}\nabla^2\varphi(\mathbf{x}, \boldsymbol{R}) = \rho(\mathbf{x}) - \sum_{I=1}^{N_a} Z_I\delta(\mathbf{x} - \boldsymbol{R}_I) \tag{2c}$$

where ψ_i denote the wavefunctions or orbitals of a material system with N_e electrons and f_i denotes the orbital occupancy given by the finite-temperature Fermi-Dirac distribution. Upon solving the above system of equations for lowest N eigenfunctions, the kinetic energy is given by $T_s(\rho) = \sum_i f(\epsilon_i)\epsilon_i - \int \rho V_{\rm eff}$. In the case of pseudopotential calculations, where only the wavefunctions for the valence electrons are computed, the Coulomb singular $V_{\rm ext}$ is replaced by a smooth pseudopotential which provides an effective potential of the nucleus and the core electrons.

1.2 Finite-element discretization

We use the finite-element (FE) basis, a C^0 continuous piecewise polynomial basis, for discretizing the Kohn-Sham Hamiltonian. The FE basis functions are local in nature and result in discrete sparse matrices, and, thus, numerical implementations based on finite-element basis scale well on massively parallel computing platforms (up to thousands of processors) and offers a distinct advantage in comparison to other widely used basis sets. The discretization of Kohn-Sham equations (2) using a finite-element basis results in a generalized eigenvalue problem given by

$$\mathbf{H}\hat{\boldsymbol{\Psi}}_i = \epsilon_i^h \mathbf{M}\hat{\boldsymbol{\Psi}}_i \ , \tag{3}$$

where H_{jk} denotes the discrete Hamiltonian matrix, M_{jk} denotes the overlap matrix and ϵ_i^h denotes i^{th} eigenvalue corresponding to the eigenvector $\hat{\boldsymbol{\Psi}}_i$ which corresponds to the nodal vector of the corresponding eigenfunction $\psi_i^h(\mathbf{x})$ on a given finite-element mesh. The sparse matrices $\mathbf{H}$ is given by

$$\mathrm{H}_{jk} = \frac{1}{2}\int \Big[\nabla N_j(\mathbf{x})\,.\nabla N_k(\mathbf{x}) + V_{\text{eff}}^h(\rho^h(\mathbf{x}), \boldsymbol{R}) N_j(\mathbf{x}) N_k(\mathbf{x})\Big]\, d\mathbf{x} \tag{4}$$

where $N_j : 1 \leq j \leq M$ denotes the finite-element basis functions and $M_{jk} = \int N_j(\mathbf{x}) N_k(\mathbf{x})\, d\mathbf{x}$ denotes the overlap matrix. The key strategies employed to improve the computational efficiency of FE discretization of Kohn-Sham equations are:

***A priori* mesh adaption:** An *a priori* mesh adaption technique is developed to construct a close to optimal FE discretization of the Kohn-Sham DFT problem by minimizing the FE approximation error in the ground-state energy for a fixed number of elements in the mesh (Motamarri et al., 2013). To achieve this, a formal bound on the approximation error is derived, as a function of mesh size, degree of FE basis functions and the electronic fields involved. This technique enables us to exploit the adaptive nature of FE basis sets by systematically coarse-graining the finite-element mesh in order to reduce the total number degrees of freedom and thereby achieve significant computational savings.

Higher-order spectral finite-elements: Higher-order spectral finite-elements up to sixth order are employed. Here the FE basis functions corresponds to Lagrange polynomials interpolated through an optimal distribution of nodes (Gauss-Lobatto-Legendre (GLL) points), corresponding to the roots of derivatives of Legendre polynomials. The use of spectral finite-elements in higher-order FE discretization of the Kohn-Sham eigenvalue problem offers two main advantages. Firstly, a spectral finite-element basis has an improved conditioning in comparison to the conventional finite-elements using equispaced nodes. Secondly, employing a GLL quadrature rule in conjunction with spectral finite-elements results in a diagonal overlap matrix which allows for trivial transformation of the generalized eigenvalue problem (3) to a standard eigenvalue problem as

$$\mathbf{H}\tilde{\boldsymbol{\Psi}}_i = \epsilon_i^h \mathbf{M}\tilde{\boldsymbol{\Psi}}_i \qquad \Rightarrow \qquad \mathbf{H}\tilde{\boldsymbol{\Psi}}_i = \epsilon_i^h \mathbf{M}^{1/2}\mathbf{M}^{1/2}\tilde{\boldsymbol{\Psi}}_i \qquad \Rightarrow \qquad \tilde{\mathbf{H}}\hat{\boldsymbol{\Psi}}_i = \epsilon_i^h \hat{\boldsymbol{\Psi}}_i \tag{5}$$

$$\text{where} \qquad \hat{\boldsymbol{\Psi}}_i = \mathbf{M}^{1/2}\tilde{\boldsymbol{\Psi}}_i; \qquad \tilde{\mathbf{H}} = \mathbf{M}^{-1/2}\mathbf{H}\mathbf{M}^{-1/2}$$

We conducted systematic studies to assess the computational efficiency afforded by higher-order FE discretizations of Kohn-Sham DFT (Motamarri et al., 2013). Our benchmark numerical studies demonstrated optimal rates of convergence for both pseudopotential as well as all-electron calculations (cf. Figures 1 & 2). While higher-order discertizations are more accurate and require lesser number of basis functions to achieve chemical accuracy in comparison to a lower-order discretization, the per basis computational cost is also higher for higher-order discretizations. Thus, in order to assess the computational efficiency of higher order finite-element discretizations we conducted a study to compare the CPU times required to compute the electronic structure of benchmark problems using various orders of finite-element basis functions. Our studies indicate that a 4th order FE basis function provides a staggering 100-1000 fold computational savings in comparison to a linear FE basis function (cf. Figures 3 & 4). This clearly demonstrates the computational efficiency afforded by higher-order discretizations in electronic structure calculations.

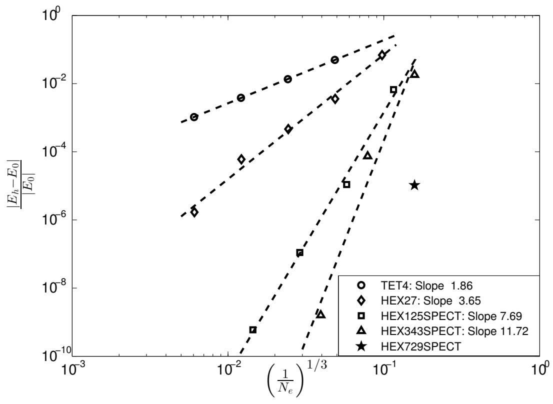

Figure 1: Convergence of error in ground-state energy of a 35-atom Barium cluster for various orders of finite-elements (pseudopotential) (Motamarri et al., 2013).

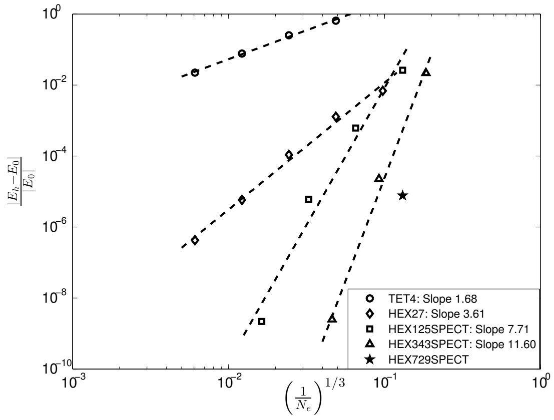

Figure 2: Convergence of error in ground-state energy of a methane molecule for various orders of finite-elements (all-electron) (Motamarri et al., 2013).

1.3 Solution of the Kohn-Sham eigenvalue problem via Chebyshev filtering:

The use of spectral elements allows us to trivially transform the generalized eigenvalue problem to a standard eigenvalue problem. Noting that the key quantity of interest in density functional theory—electron-density—can be computed from the eigenspace of the occupied states, we employ the Chebyshev filtering technique (ChFSI-FE) to compute an approximation to the occupied eigenspace. We refer to Motamarri et al. (2013); Motamarri & Gavini (2014) for the specific details of our implementation. In brief, the ChFSI technique represents a modified power iteration in every SCF iteration that exploits the rapid growth of Chebyshev polynomials in $(-\infty, -1)$ to magnify the relevant eigenspectrum (Zhou et al., 2006), thus providing a good subspace for the solution of the Kohn-Sham eigenvalue problem. Upon computing the Chebyshev filtered subspace, we orthogonalize the Chebyshev filtered vectors and project the discrete Hamiltonian onto the subspace and compute the eigenvalue and eigenvectors of the subspace projected Hamiltonian. We evaluated the efficiency of the ChFSI-FE approach with conventional approaches of solving the generalized Kohn-Sham eigenvalue problem using Jacobi-Davidson method and the standard eigenvalue problem using the Krylov Schur method. Table 1 shows this comparison demonstrating the significant computational efficiency afforded by ChFSI-FE for both pseudopotential and all-electron calculations.

Table 1: Comparison of generalized eigenvalue problem, standard eigenvalue problem, and the Chebyshev filtering technique. Benchmark problems include an all-electron calculation of 16 atom graphene sheet and a pseudopotential calculation on a 172 atom aluminum cluster (Motamarri et al., 2013).

Element Type	DOFs	Problem Type	N	Time (GHEP)	Time (SHEP)	ChFSI-FE
HEX125SPECT	1,368,801	graphene	96	1786 CPU-hrs	150 CPU-hrs	12.5
HEX343SPECT	2,808,385	Al $3 \times 3 \times 3$ cluster	516	2084 CPU-hrs	80 CPU-hrs	13

We also conducted benchmark studies comparing the developed approach using ChFSI-FE with ABINIT software, which is a well developed plane-wave based method for solving the ground-state

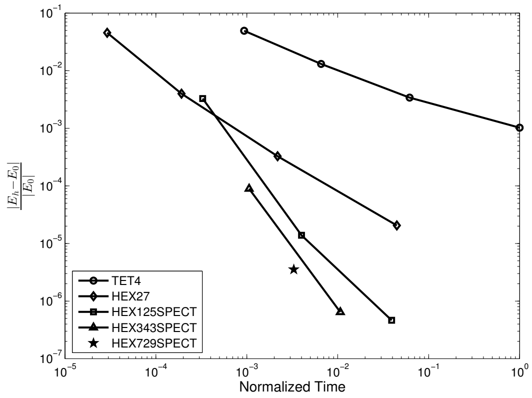

Figure 3: Relative performance of various orders of finite-elements measured in terms of computational time for pseudopotential calculation of 35-atom Barium cluster (Motamarri et al., 2013).

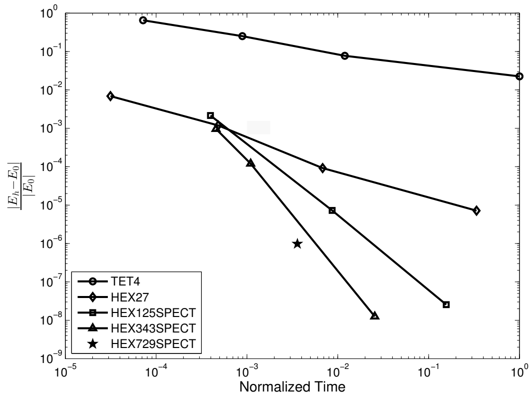

Figure 4: Relative performance of various orders of finite-elements measured in terms of computational time for the all-electron calculation of methane molecule (Motamarri et al., 2013).

Kohn-Sham DFT problem. Table 2 shows these results which demonstrates a significant outperformance by the developed approach. Using the developed real-space approach, we have demonstrated pseudopotential calculations on systems as large as a few thousand atoms and all-electron calculations on systems as large as a few thousand electrons using the modest computational resources at our disposal. Figures 5 & 6 show the electron density contours from all-electron calculations of a graphene sheet contating 100 atoms and Tris (bipyridine) ruthenium complex, an organo-metallic complex. Further, given the good scaling exhibited by the developed implementation on parallel computing architectures (cf. Figure 7), systems beyond the reach of conventional plane-wave based implementations are now accessible.

Table 2: Comparison of the developed real-space DFT code with ABINIT for an Aluminum nanocluster containing 666 atoms (pseudopotential calculation with Troullier Martins psedopotential).

Type of basis set	Energy (eV) per atom	Abs. error (eV) per atom	Rel. error	Time (CPU-hrs)
ABINIT (cut-off 20 Ha; $1,093,421$ plane waves)	-56.8739	0.0043	7.5×10^{-5}	8640
Real-space (HEX343SPECT FE basis; $4,363,621$ nodes)	-56.8765	0.0017	3×10^{-5}	1132

2 Reduced order scaling using localization ideas and quasi-continuum reduction:

The real-space ChFSI-FE formulation discussed in the previous section, which computes the canonical eigenfunctions and eigenvalues, asymptotically scales cubically with number of atoms (due to the cubic scaling of diagonalizing a matrix). This becomes prohibitively expensive for large-scale DFT calculations, and hence, in order to reduce the computational complexity, we developed a subspace projection technique (Motamarri & Gavini, 2014) that has reduced order scaling. The formulation

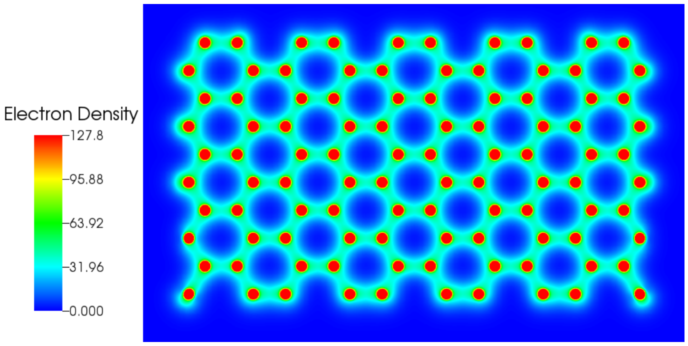

Figure 5: Electron-density contours from an all-electron DFT calculation of a 100 atom graphene sheet (Motamarri et al., 2013).

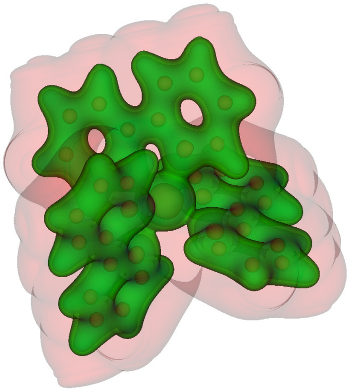

Figure 6: Isocontours of the electron density from an all-electron calculation of Tris (bipyridine) ruthenium complex (Motamarri et al., 2013).

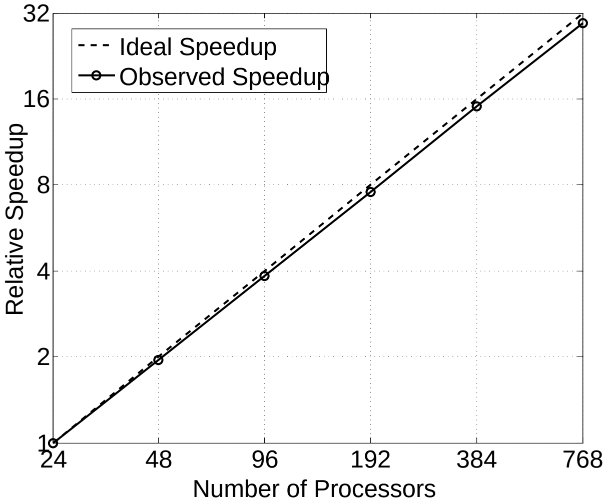

Figure 7: Strong scaling study demonstrating over 90% efficiency at 768 processors. Benchmark system is 3 × 3 × 3 aluminum cluster (172 atom) with a FE discretization containing 4 million basis functions.

provides a *single unified framework to handle both insulating and metallic systems*. Further, both pseudopotential as well as all-electron calculations can be conducted using the proposed methodology. The key ideas involved in the method include: (i) expressing the Kohn-Sham Hamiltonian and the corresponding wave-functions in Löwdin orthonormalized finite-element basis constructed using spectral finite-elements in conjunction with GLL quadrature rules; (ii) employing a Chebyshev filtering approach in each SCF iteration for an efficient computation of the eigenspace; (iii) use a localization procedure (Garcia-Cervera et al., 2009) to compute atom-centered nonorthogonal localized basis (localized wavefunctions) spanning the Chebyshev filtered subspace; (iv) computing the projection of the Hamiltonian into the non-orthogonal localized basis and using a Fermi-operator (Baer & Head-Gordon, 1997) expansion of the projected Hamiltonian to compute the relevant quantities like density matrix, electron density and the band energy. The computational complexity of this algorithm for well-localized wavefunctions with a compact support is shown to be linear – $\mathcal{O}(N)$. We refer to Motamarri & Gavini (2014) for details of this algorithm, and present here some benchmark results that demonstrates the significant computational efficiency afforded by this approach. Figure 8 shows the computational time per SCF for the developed subspace projection method in comparison with ChFSI-FE for benchmark problems involving a series aluminum nano-clusters and alkane chains. As is evident the developed localization approach provides close to ten-fold computational savings and enables consideration of systems approaching close to 10,000 atoms. Further, we note that the observed scaling for the alkane chains (system with band gap) is close to linear scaling with system size, and the scaling for aluminum clusters (representative of a metallic system) is $\sim O(N^{1.5})$, which is a significant improvement over the cubic-scaling for conventional solution methods.

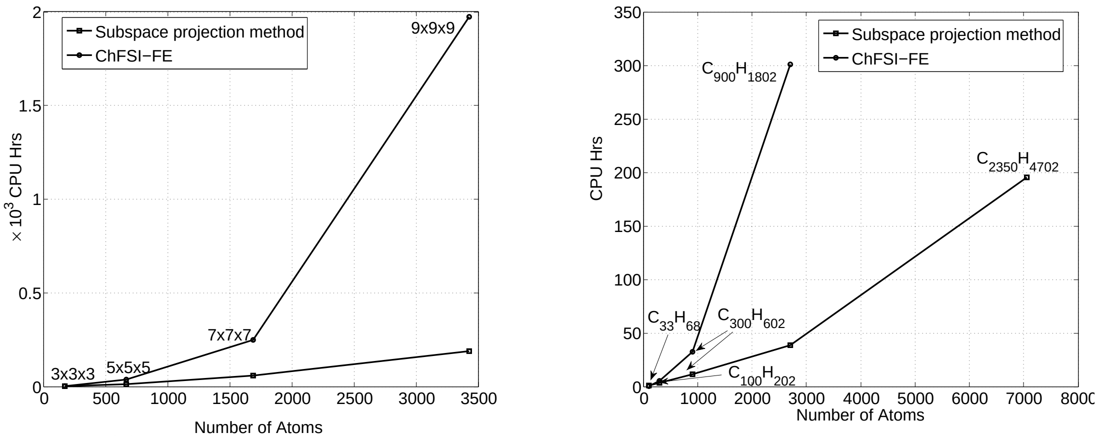

(a) Metallic system (b) Insulating system

Figure 8: Average computational time (CPU-Hrs) per SCF iteration for the subspace projection method and ChFSI-FE for a pseudopotential calculation. Case study: (a) Aluminum nano-clusters(upto 3430 atoms) (b) Alkane chains (up to 7000 atoms) (Motamarri & Gavini, 2014).

While providing reduced order scaling, the developed localization technique is also crucial to the quasi-continuum reduction of Kohn-Sham DFT. Using this localized representation, the wavefunctions are decomposed into a predictor and corrector, where the predictor is computed using the Cauchy Born hypothesis (along the similar lines as the quasi-continuum reduction for orbital-free DFT (Gavini et al., 2007; Radhakrishnan & Gavini, 2010)). In regions of smooth deformations, such as away from the defect-core, the predictor provides an effective representation of the wavefunction, whereas in regions close to the defect-core the corrector provides corrections to the predictor. Given the nature of the corrector fields, they can be efficiently represented by using an adaptive discretization, with more resolution near the defect-core and coarse-graining away from it. We are currently implementing the quasi-continuum reduction for Kohn-Sham DFT using the localization technique in our framework.

3 Application studies:

We investigated the energetics of point defects—monovacancy, self-interstitials (tetrahedral, octahedral and dumbbell) and Frenkel pairs—in aluminum under tensile hydrostatic stresses in order to understanding the mechanisms leading to spall failure in metals. We find that that the defect core-energy of a vacancy, which is governed solely by the electronic-structure at the core, significantly depends on the macroscopic hydrostatic stress, and that this constitutes an important contribution to the formation enthalpy, especially in the regime of extreme tensile hydrostatic stresses. This finding is in contrast to widely used elastic formulations of point defects based on formation volume that ignore the defect core-energy contribution. The formation enthalpies of all point defects considered in this study monotonically decrease with increasing tensile hydrostatic stress (cf. Figure 9). Further, we find that the formation enthalpies of vacancies and Frenkel pairs are negative beyond critical tensile hydrostatic stresses (9 GPa for vacancies and 12 GPa for Frenkel pairs), which suggests a spontaneous nucleation of these point defects and this has important implications to nucleation mechanisms leading to spall failure. In particular, these findings suggest two possible defect nucleation mechanisms leading to spall failure: (i) a heterogeneous nucleation of vacancies from defect sources; (ii) a homogeneous nucleation of Frenkel pairs at higher hydrostatic stresses. We refer to (Iyer et al., 2014) for further details on the calculations and the findings.

4 Publications supported by this grant

1 Motamarri, P., Nowak, M.R., Leiter, K., Knap, J., Gavini, V., Higher-order adaptive finite-element methods for Kohn-Sham density functional theory, *J. Comput. Phys.* **253**, 308-343 (2013).

2 Iyer, M., Pollock, T.M., Gavini, V., Energetics and nucleation of point defects in aluminum under extreme tensile hydrostatic stresses, *Phys. Rev. B* **89**, 014108 (2014).

3 Motamarri, P., Gavini, V., A subquadratic-scaling subspace projection method for large-scale Kohn-Sham DFT calculations using spectral finite-element discretization, *Phys. Rev. B* **90**, 115127 (2014).

4 Motamarri, P., Blesgen, T., Gavini, V., Tucker-tensor algorithm for large-scale Kohn-Sham density functional theory calculations, *Phys. Rev. B* **93**, 125104 (2016).

5 Motamarri, P., Gavini, V., Configurational forces in electronic structure calculations (in preparation, 2016).

6 Motamarri, P., Gavini, V., Bhattacharya, K., Ortiz, M., A spectrum splitting approach for large-scale all-electron Kohn-Sham DFT calculations (in preparation, 2016).

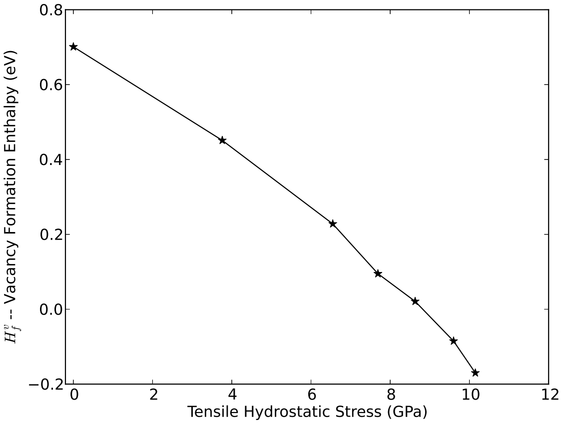

(a) Vacancy

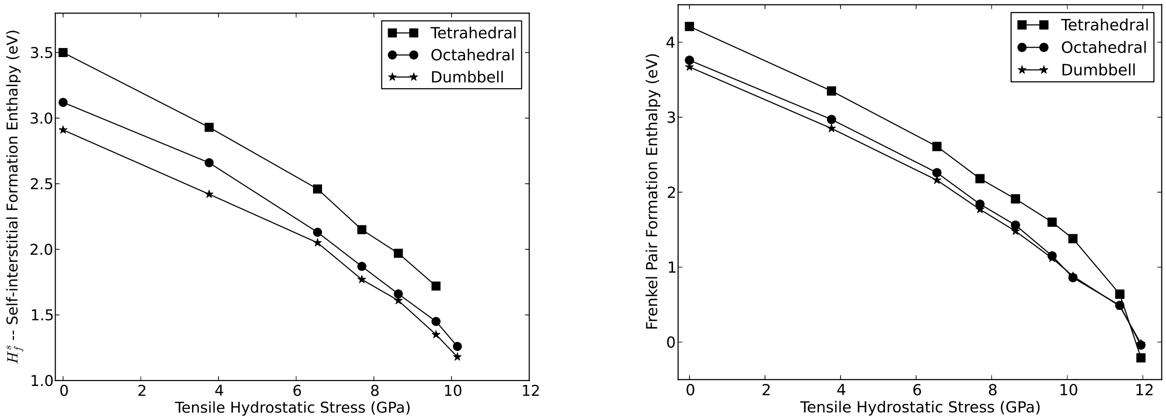

(b) Self interstitial

(c) Frenkel pair

Figure 9: Formation enthalpies of point defects as a function of tensile hydrostatic stress (Iyer et al., 2014).

References

Baer. R., Head-Gordon, M., Chebyshev expansion methods for electronic structure calculations on large molecular systems, *J. Chem. Phys.*, **107** 10003-10013 (1997).

Garcia-Cervera, C.J., Lu, J., Xuan, Y., E, W., Linear-scaling subspace-iteration algorithm with optimally localized nonorthogonal wave functions for Kohn-Sham density functional theory. *Phys. Rev. B*, **79** 115110, (2009).

Gavini, V., Bhattacharya, K., Ortiz, M., Quasi-continuum orbital-free density-functional theory: A route to multi-million atom non-periodic DFT calculation, *J. Mech. Phys. Solids* **55**, 697 (2007).

Iyer, M., Pollock, T.M., Gavini, V., Energetics and nucleation of point defects in aluminum under extreme tensile hydrostatic stresses, *Phys. Rev. B* **89**, 014108 (2014).

Motamarri, P., Iyer, M., Knap, J., Gavini, V., A numerical analysis of the finite-element discretization of orbital-free density functional theory, *J. Comp. Phys.* **231**, 6596-6621 (2012)..

Motamarri, P., Nowak, M.R., Leiter, K., Knap, J., Gavini, V., A higher order adaptive finite-element discretization of Kohn-Sham density functional theory, *J. Comput. Phys.* **253**, 308-343 (2013).

Motamarri, P., Gavini, V., A subquadratic-scaling subspace projection method for large-scale Kohn-Sham DFT calculations using spectral finite-element discretization, *Phys. Rev. B* **90**, 115127 (2014).

Motamarri, P., Blesgen, T., Gavini, V., Tucker-tensor algorithm for large-scale Kohn-Sham density functional theory calculations, *Phys. Rev. B* **93**, 125104 (2016).

Radhakrishnan, B.G., Gavini, V., Effect of cell size on the energetics of vacancies in aluminum studied via orbital-free density functional theory, *Phys. Rev. B* **82**, 094117 (2010).

Zhou, Y., Saad, Y., Tiago, M.L., Chelikowsky, J.R., Parallel self- consistent-field calculations via Chebyshev-filtered subspace acceleration *Phys. Rev. E*, **74** 066704, (2006).

1.

1. Report Type

Final Report

Primary Contact E-mail
Contact email if there is a problem with the report.

vikramg@umich.edu

Primary Contact Phone Number
Contact phone number if there is a problem with the report

734-763-9685

Organization / Institution name

University of Michigan

Grant/Contract Title
The full title of the funded effort.

Quasi-continuum reduction of field theories: A route to seamlessly bridge quantum and atomistic length-scales with continuum

Grant/Contract Number
AFOSR assigned control number. It must begin with "FA9550" or "F49620" or "FA2386".

FA9550-13-1-0113

Principal Investigator Name
The full name of the principal investigator on the grant or contract.

Vikram Gavini

Program Manager
The AFOSR Program Manager currently assigned to the award

Dr. Jean-Luc Cambier

Reporting Period Start Date

03/01/2013

Reporting Period End Date

02/29/2016

Abstract

This report summarizes the research objectives achieved in this project during the period 03-01-2013 to 02-29-2016. Computational techniques have been developed that enable large-scale real-space electronic structure calculations using Kohn-Sham density functional theory. In particular, the various components of the developed techniques include (i) real-space formulation of Kohn-Sham density-functional theory (DFT) for both pseudopotential and all-electron calculations based on a finite-element discretization; (ii) development of efficient and scalable algorithms for the solution of the Kohn-Sham eigenvalue problem based on Chebyshev filtering; (iii) development of reduced- order scaling techniques by employing a subspace projection technique in conjunction with local- ization techniques that construct a non-orthogonal localized basis spanning the Chebyshev filtered subspace; (iv) leveraging the localized representation to construct the quasi-continuum reduction. Most aspects of these developments have been numerically implemented, and the benchmark stud- ies have demonstrated that the developed techniques significantly outperform existing conventional DFT implementations in terms of computational efficiency, scaling with system size, and parallel scalability of the numerical implementation. We believe these developed techniques and the numeri- cal implementation can aid as a platform for further development of scalable and efficient real-space Kohn-Sham DFT calculations on tens of thousands of atoms, and enable

continuing efforts towards a seamless bridging of the quantum and continuum length-scales.

Distribution Statement

This is block 12 on the SF298 form.

Distribution A - Approved for Public Release

Explanation for Distribution Statement

If this is not approved for public release, please provide a short explanation. E.g., contains proprietary information.

SF298 Form

Please attach your SF298 form. A blank SF298 can be found here. Please do not password protect or secure the PDF The maximum file size for an SF298 is 50MB.

SF298_Final.pdf

Upload the Report Document. File must be a PDF. Please do not password protect or secure the PDF . The maximum file size for the Report Document is 50MB.

FinalReport.pdf

Upload a Report Document, if any. The maximum file size for the Report Document is 50MB.

Archival Publications (published) during reporting period:

1. Motamarri, P., Nowak, M.R., Leiter, K., Knap, J., Gavini, V., Higher-order adaptive finite- element methods for Kohn-Sham density functional theory, J. Comput. Phys. 253, 308-343 (2013).

2. Iyer, M., Pollock, T.M., Gavini, V., Energetics and nucleation of point defects in aluminum under extreme tensile hydrostatic stresses, Phys. Rev. B 89, 014108 (2014).

3. Motamarri, P., Gavini, V., A subquadratic-scaling subspace projection method for large-scale Kohn-Sham DFT calculations using spectral finite-element discretization, Phys. Rev. B 90, 115127 (2014).

4. Motamarri, P., Blesgen, T., Gavini, V., Tucker-tensor algorithm for large-scale Kohn-Sham den- sity functional theory calculations, Phys. Rev. B 93, 125104 (2016).

5. Motamarri, P., Gavini, V., Configurational forces in electronic structure calculations (in preparation, 2016).

6. Motamarri, P., Gavini, V., Bhattacharya, K., Ortiz, M., A spectrum splitting approach for large-scale all-electron Kohn-Sham DFT calculations (in preparation, 2016).

Changes in research objectives (if any):

Change in AFOSR Program Manager, if any:

Dr. Jean-Luc Cambier

Extensions granted or milestones slipped, if any:

AFOSR LRIR Number

LRIR Title

Reporting Period

Laboratory Task Manager

Program Officer

Research Objectives

Technical Summary

Funding Summary by Cost Category (by FY, $K)

	Starting FY	FY+1	FY+2
Salary			
Equipment/Facilities			
Supplies			
Total			

Report Document

Report Document - Text Analysis

Report Document - Text Analysis

Appendix Documents

2. Thank You

E-mail user

Apr 01, 2016 13:11:16 Success: Email Sent to: vikramg@umich.edu